Korean J. Chem. Eng., **28**(5), 1280-1285 (2011)
DOI: 10.1007/s11814-010-0489-8

Kinetics and optimization of L-tryptophan separation with ion-exchange chromatography

Wei Luo*, Peilian Wei, Hao Chen*, Limei Fan***, Lei Huang*,†, Jin Huang*, Zhinan Xu*, and Peilin Cen***

*Institute of Bioengineering, Department of Chemical and Biological Engineering,
Zhejiang University, Hangzhou 310027, China
**School of Biological and Chemical Engineering, Zhejiang University of Science and Technology, Hangzhou 310012, China
***Zhejiang University City College, Hangzhou 310015, China
(*Received 7 July 2010 • accepted 19 November 2010*)

Abstract−Adsorption and desorption of L-tryptophan (L-trp) on strong acid cation exchange resin were investigated in a fixed-bed column. L-trp was effectively adsorbed onto the resin HZ-001, with the loading capacity and breakthrough time determined. Four kinetic models, including Adams-Bohard, Wolborska, Thomas, and Yoon-Nelson models, were adopted to determine the kinetic parameters of adsorption and to predict the breakthrough curves. The results showed that the models used described the breakthrough well. Desorption of L-trp from the column bed was performed using aqueous ammonia as the eluant. Optimum procedure was obtained with 2.0 M aqueous ammonia at the elution velocity of 6 BV/h. Five cycles of adsorption-elution-regeneration were conducted to evaluate the column reutilization.

Key words: L-tryptophan, Adsorption, Elution, Kinetics, Optimization

INTRODUCTION

As an amphoteric substance, L-trp exists as anions or cations depending on the pH value of the solution, which offers a basis for the separation of L-trp by ion exchange process. Below the pH value of 5.89 (pKa of L-trp, 25 °C), L-trp is positively charged and can be easily taken up onto a cation exchanger. While the solution pH is changed to alkalescence, the negatively charged L-trp can be desorbed from the cation exchanger. Such characteristics enable the concentration and recovery of L-trp through a cyclic operation with the alteration of solution pH.

Ion exchange technology has been extensively studied and widely applied in various separation processes [1,2]. Ion exchangers, such as ion exchange resin, are solid and insoluble high molecular weight polyelectrolytes that carry functional groups and exchange ions. Due to high-efficiency, low cost, and reutilization of ion exchange resins, they have a wide application in scientific research, industrial production and other processes [3-6]. The ion exchange process is usually operated in a packed bed in an industrial separation process. A packed bed column is an effective process for cyclic adsorption/desorption, as it makes the best use of the physical sorption, chemical ion-exchange and other mechanisms known to be a driving force for adsorption and allows more efficient utilization of the sorbent capacity and recycle. Some primary work has been performed to separate L-trp from L-serine and indole mixtures with the neutral polymeric resins XAD-4 and XAD-7 in the successive column system [7]. Köse and Öztürk have utilized a strong base anion-exchange resin (Dowex 2×8) in a packed column for the removal of boron from aqueous solutions [8]. Alguacil et al. have also reported Chromium (III) recovery from waste acid solution by ion exchange resin (Amberlite IR-120) and modeled the column exchange behavior [9]. To design a separation procedure for an adsorbate, it is important to understand the loading capacities and adsorption kinetics as well as elution characteristic between the adsorbent and adsorbate. The breakthrough curve and the adsorption equilibrium are perhaps the most common basis for assessing the behavior of the adsorption process [10-12].

In our previous work, one strong cation resin (HZ-001) was screened out for its good performance for L-trp separation [13]. Further work was carried out to investigate the column performances of the strong cation resin HZ-001 for the adsorption of L-trp from the aqueous solution. The results were fitted by several kinetic models to predict the breakthrough curves and to determine the parameters of column performance for process design. The elution process of the adsorbed solutes in the column was optimized by the kinetic characteristics.

MATERIALS AND METHODS

HZ-001 [13], is a strong acid cation exchange resin and its characteristics are listed in Table 1. Before use, HZ-001 was washed with

Table 1. Typical chemical and physical characteristics of HZ-001 ion exchange resin[a]

Constitutional type	Microporous
Polymer matrix	Styrene-DVB
Functional group	Sulfonic acid
Ionic form	Na^+
Particle size (mesh)	100-200
Moisture content (%)	43-53
Wet apparent density (g/mL)	0.80-0.90
Total exchange capacity (mM/g)	≥4.2
(mM/mL)	≥1.7

[a]Information provided by the manufacturer

†To whom correspondence should be addressed.
E-mail: lhuangblue@zju.edu.cn

distilled water several times, then washed with 1.5 M NaOH and HCl alternately, and finally washed by double-distilled water to around pH 7.0 for use.

L-trp (purity ≥99.5%), purchased from Sigma (St. Louis, US), was used in the study and its aqueous solution (10.0 g/L, pH 5.0) was prepared for the column adsorption. Column studies were conducted using a glass column with an inner diameter of 1.0 cm and a length of 20.0 cm. The column was packed with 10.0 g of HZ-001 that was wet-settled beforehand and the air bubbles in the column were excluded outside. The aqueous solution was loaded onto the column at a desired flow rate using a peristaltic pump. Aliquots of 1.0 mL of the effluent were collected with a fraction collector for the solution titer analysis. A breakthrough curve was determined after the UV spectrophotometer assay for L-trp. When the effluent concentration of the adsorbate reached the influent concentration (i.e., 100% of breakthrough), the column process was terminated.

The elution step began after the column was washed with 2 bed volume of double-distilled water. Aqueous ammonia (0.5, 1.0, 2.0 M) was used as the eluant. Preliminary experiments were conducted to determine the flow rate. Crystallization of amino-L-trp formed markedly at low flow rates (below 0.375 mL/min), leading to the column blockage. The elution profile was obtained with the analysis of each fraction collected by the fraction collector.

Adsorption and desorption procedures were repeated to evaluate their practical application. The reutilization studies were conducted by five cycles of adsorption and elution. The L-trp solution with a feed concentration of 10.0 g/L was loaded on the column at 1.2 mL/min. Subsequently, the adsorbed L-trp was eluted by 2.0 M aqueous ammonia. When the effluent concentration became nearly zero, distilled water was introduced into the column to wash out aqueous ammonia followed by the regeneration with 1.0 M HCl for the next adsorption process.

RESULTS AND DISCUSSION

1. Adsorption of L-trp in Fixed Bed Column

The column performance is usually evaluated by loading capacity and adsorption kinetics through the concept of the breakthrough curve. The breakthrough curve shows the loading behavior of adsorbate in a fixed bed since the breakthrough time and the shape of the breakthrough curve are of importance in determining the loading capacity and dynamic response for the column process. A breakthrough curve is often represented in terms of adsorbed substance concentration or normalized concentration defined as the ratio of effluent concentration to inlet substance concentration (C_e/C_0) as a function of flow time (t) or volume of effluent (V_e). For an ideal adsorption process, the breakthrough curve should be a step function characterized by an instantaneous jump in the effluent concentration from zero to the influent concentration at the moment the column is saturated [14-16].

In the present study, the breakthrough time (t_b) was defined as the time at which the effluent concentration arrived at approximately 1% of the influent concentration (C_e/C_0=0.01), which represented the time that the column was still active, while the bed exhaustion time (t_e) was defined as the time required to reach the exhaust point (C_e/C_0=0.99). The mass transfer zone (MTZ), one of the parameters frequently employed to determine the effective height of the adsorption column, was then evaluated based on the value of Δt (Δt=t_e−t_b), and the length of bed column and was expressed in the following form:

$$MTZ = \frac{L\Delta t}{t_e} \quad (1)$$

where L refers to the bed height (cm). The loading capacity of the fixed bed can be determined by the integrating adsorbed concentration versus the throughput volume from the breakthrough curve and is expressed as follows [17]:

$$q_e = \int_0^{V_t} \frac{(C_0 - C_e)dV}{m} \quad (2)$$

where q is the loading capacity (mg/g) as a function of adsorbate concentration and flow rate; C_0 and C_e are the inlet adsorbate concentration and effluent concentration at equilibrium, respectively; V is the effluent volume (mL); m is the mass of the adsorbent (g). Contact time is also an important parameter in the design of fixed bed system and is usually expressed in terms of empty bed contact time (EBCT). EBCT affects the breakthrough volume and the profile of breakthrough curve, expressed as the following form:

$$ECBT = \frac{V_b}{Q} \quad (3)$$

The performance of a fixed bed can be further evaluated in terms of adsorbent usage rate, U_r and it is given:

$$U_r = \frac{m}{V} \quad (4)$$

where V_b is the volume of adsorbent in the fixed bed (mL); Q, the flow rate (mL/min); V, the solution volume at breakthrough (mL).

Fig. 1 shows the breakthrough profiles for the adsorption of L-trp in the packed bed at different flow rates. As indicated in Fig. 1, the sharpness of the breakthrough curve increased with the increasing flow rate from 1.182 to 1.348 mL/min, while the profiles were close to each other when the flow rates were set at 0.962 and 1.182 mL/min. The curves exhibited a broader tailing edge at low flow rate. The breadth of the tailing edge is most probably determined by the slow intraparticle diffusion of L-trp within HZ-001. Cooney

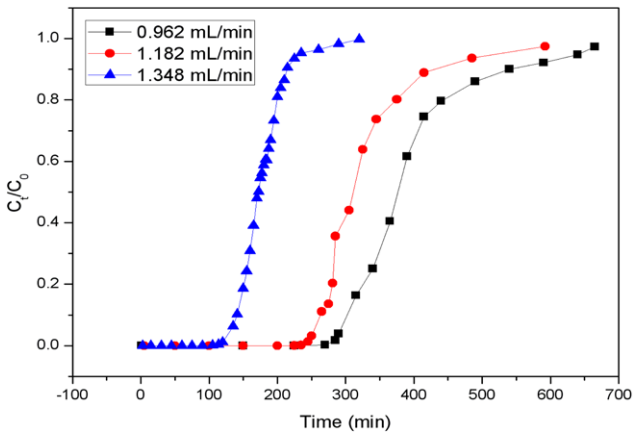

Fig. 1. Breakthrough curves for L-trp adsorption on HZ-001 packed column.

Table 2. Column performance of HZ-001 at different flow rates

Flow rate (mL/min)	t_b (min)	t_e (min)	Δt (min)	MTZ (cm)	EBCT (min)	U_r (g/L)	q_e (mg/g)
0.962	285	665	380	10.9	15.6	19.2	705.8
1.182	245	592	347	11.1	12.7	18.2	672.7
1.348	120	320	200	11.9	11.1	33.0	405.8

has demonstrated that the "tailing" of a breakthrough curve (i.e., a slow approaching of C_e/C_0 to 1.0) is commonly observed in a liquid-phase adsorption system within which the transport process is dependent on the intraparticle diffusion [18].

It can be observed from Fig. 1 that the breakthrough/exhaustion time decreased with the increase of flow rate. As shown in Table 2, the breakthrough time and exhaustion time were reduced by 57.9% and 51.9%, respectively, along with a reduction of 42.5% in the loading capacity of column bed when the flow rate was increased from 0.962 to 1.348 mL/min. The result indicated that the adsorption capacity may increase with decreasing flow rate or increasing EBCT. This behavior can be explained by the fact that the L-trp adsorption is affected by insufficient residence time of L-trp in the column bed. This insufficient residence time resulted in non-complete ion exchange between solute and resin, thus decreasing the adsorption performance of the column bed.

The values of EBCT and U_r were determined from the breakthrough and the results were listed in Table 2. It shows that the U_r values were close to each other with the EBCT increasing from 12.7 to 15.6 min, while sharply enhanced to 33.0 g/L when the EBCT was reduced to 11.1 min. This indicated that the ideal contact time in the column should not be less than 12.7 min in order to maintain the lowest usage rate in this study (around 19 g/L).

MTZ is formed at the front of the column where adsorption takes place. Thereafter, MTZ moves down through the adsorbent bed until it reaches the adsorbent end, where the effluent concentration of solute begins to rise in the aqueous phase. The length of MTZ has been considered as a critical bed depth (CBD), which represents a band between adsorbent and adsorbate. CBD is defined as the minimum bed depth required to obtain the breakthrough at t=0. It was observed that MTZ increased with the increase of flow rate (Table 2). The results indicated that the column performance was of inverse-correlation with MTZ. At higher flow rate, the rate of mass transfer tends to increase. The amount of L-trp adsorbed onto the unit bed height (mass transfer zone) increased with the increase of flow rate, which led to faster saturation.

2. Modeling of Breakthrough Curves

Ion exchange is usually a complex process whose performance is affected by a number of parameters, such as the equilibrium loading capacity and the mass transfer rate [19]. Accurate prediction of column performance is difficult sometimes as this assignment includes the resolution of a set of non-linear partial differential equations by sophisticated numerical schemes with proper process parameters. However, as an alternative, several macroscopic models were proposed for describing the solute breakthrough behavior of a column adsorber [9,17,20,21]. The main advantages of these models rely on their simplicity and reasonable accuracy in the application of predicting the breakthrough time and mass transfer coefficient.

Table 3. Parameters predicted from the Adams-Bohart and Wolborska models

Flow rate (mL/min)	Adams-Bohart model		Wolborska model	R^2
	K_{AB} (mL g^{-1} min^{-1})	N_0 (g L^{-1})	β_a (min^{-1})	
0.962	5.89	233.9	1.38	0.912
1.182	9.16	237.2	2.17	0.922
1.348	10.38	153.2	1.59	0.955

2-1. Application of the Adams-Bohart and the Wolborska Models

Although originally used for the gas-charcoal adsorption study, the Adams-Bohart model has been validated in other adsorption systems [12,22,23]. The model assumes that the adsorption rate is proportional to both the loading capacity of the adsorbent and the concentration of adsorbate. The model is applied to describe the initial data of breakthrough curve and is expressed as follows:

$$\mathrm{Ln}\frac{C_t}{C_0} = K_{AB}C_0 t - \frac{K_{AB}N_0 Z}{U_0} \quad (5)$$

where C_t is the effluent adsorbate concentration at time t (mg/L); K_{AB}, the kinetic constant (mL g^{-1} min^{-1}); N_0, the saturation concentration (mg/L); Z, the column length (cm); U_0, the superficial flow rate (cm/min).

Similar to the expression of Adams-Bohart model, the Wolborska model is usually applied for the adsorption kinetics using mass transfer equations for diffusion mechanisms. By replacing KAB with β/N_0, the Wolborska equation is obtained:

$$\mathrm{Ln}\frac{C_t}{C_0} = \frac{\beta C_0 t}{N_0} - \frac{\beta Z}{U_0} \quad (6)$$

where β is kinetic constant of the external mass transfer (min^{-1}).

The kinetic parameters of both models along with the correlation coefficients, listed in Table 3, were determined from the plot of $\mathrm{Ln}C_t/C_0$ against time t at a given flow rate. The breakthrough data of relative concentration ratio (C_t/C_0) lower than 0.5 were adopted for the model fit. It appears that the overall kinetic parameters were markedly influenced by flow rate, indicating that the general adsorption process of the initial part of breakthrough process was controlled by external transfer coefficient. The maximum adsorption capacity (N_0) was also significantly affected by flow rate from 1.182 mL/min to 1.348 mL/min. This was attributed to shorter residence time of L-trp in fixed bed for adsorption onto HZ-001 at higher flow rate, thus resulting in reduction in the column performance as a function of flow rate. The column performance attained a maximum at 1.182 mL/min since the N_0 value did not increase with the decreasing flow rate. The kinetic parameter β was used to describe the mass transfer in liquid phase and axial dispersion. As shown in Table 3, β value increased first and decreased as a function of flow rate, which indicated that another mechanism also affected the mass transfer of adsorbate in addition to flow rate. The correlation coefficients (R^2) in Table 3 show that there was a good agreement between the experimental and predicted values, suggesting that both the Adams-Bohart and Wolborska models were valid for the relative concentration region up to 0.5 where large discrepancies were found between the experimental and predicted curves above this level.

2-2. Application of the Thomas and the Yoon-Nelson Models

The column data were fitted by the Thomas and the Yoon-Nelson models as well. The main advantages of the two models are dependent on their simplicity and accuracy in predicting the breakthrough curve under various operating conditions [20]. The Thomas model is a famous and widely used method in column adsorption for the determination of the maximum loading capacity, an important parameter in the design of fixed bed:

$$\mathrm{Ln}\left(\frac{C_0}{C_t}-1\right)=-K_{Th}C_0t+\frac{K_{Th}q_mX}{Q} \quad (7)$$

where K_{Th} is the Thomas rate constant (L min^{-1} g^{-1}); q_m, the loading capacity of the fixed bed (mg/g); X, the mass of adsorbent (g).

The Yoon-Nelson model was first applied to investigate the adsorption and breakthrough of adsorbate vapors or gases with respect to activated charcoal [24]. It has been extensively applied in the description of adsorption and breakthrough behavior in fixed beds regardless of the properties of adsorbate, adsorbent and information of the fixed bed [11,25,26]. The Yoon-Nelson equation pertaining to a single-component system has the following form:

$$\mathrm{Ln}\left(\frac{C_0}{C_t}-1\right)=-K_{YN}(t-\tau) \quad (8)$$

where K_{YN} is the Yoon-Nelson rate constant (min^{-1}); τ, the time required for 50% breakthrough of absorbate (min). A practical application of the experimental breakthrough curves is the determination of the breakthrough time, which is useful in establishing the optimum operating conditions for the ion exchange process. The Yoon-Nelson model can solve the problem by determination of τ value using linear regression. In fact, the above two equations are essentially the same. A comparison of Eq. (4) and Eq. (5) reveals that $K_{YN}=K_{Th}C_0$ and $\tau=q_mX/(QC_0)$.

A linear regression was then conducted on $\mathrm{Ln}(C_0/C_t-1)$ versus t to determine the parameters from the slope and intercept. The parameters along with correlation coefficients are listed in Table 4. As the flow rate increased, the Thomas rate constant K_{YN} and Yoon-Nelson constants increased, indicating they were dependent on the flow rate. The bed capacity parameters (q_m) decreased with the increasing flow rate, since lower flow rate permitted longer time for the contact of L-trp solution with bed resins. The τ value calculated based on the Yoon-Nelson model decreased by 54.4% when the flow rate was increased from 0.962 mL/min to 1.348 mL/min, which is significantly affected by the flow rate. However, the bed capacity only decreased by 0.8% by the prediction of the equation, compared with the 19.3% reduction in the 50% breakthrough time (τ_{the}) when the flow rate changed from 0.962 mL/min to 1.182 mL/min. The aforementioned determination of 50% breakthrough time is of significance as the adsorption rate and period should be considered in the actual design of the adsorption system. The calculated bed capacity (q_{the}) and 50% breakthrough time (τ_{the}) are close to the actual results, which demonstrated that the models used were accurate and valid in this

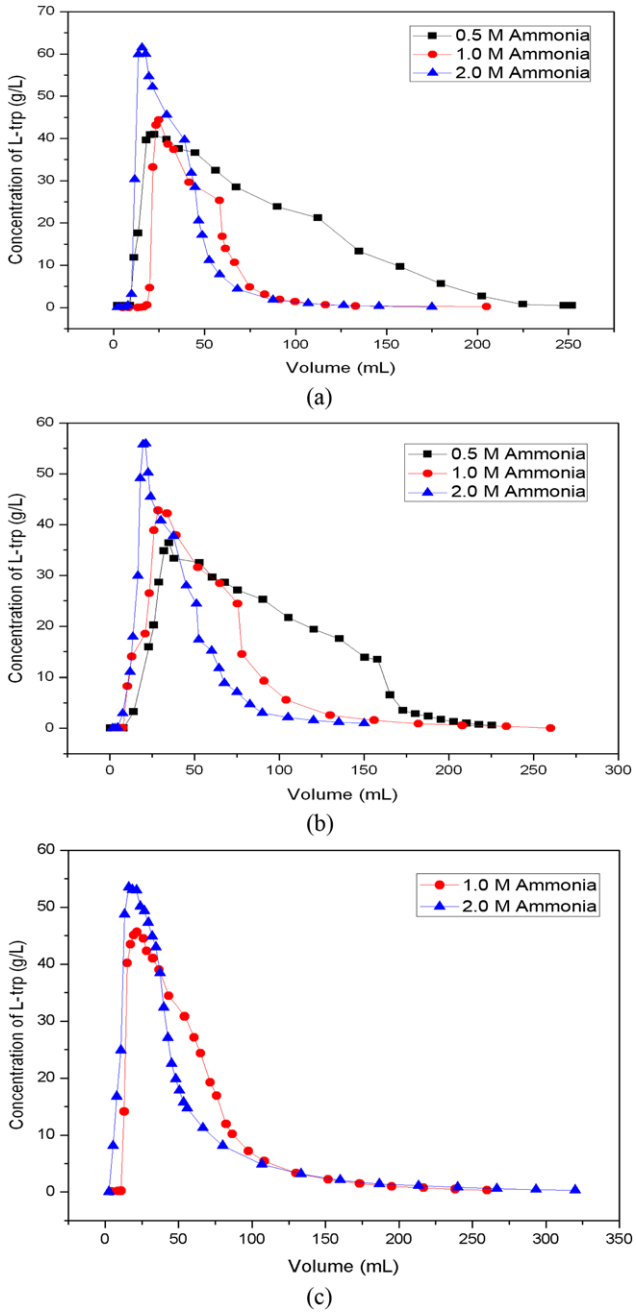

Fig. 2. Desorption profiles of L-trp at different flow rates: (a) 3 BV/h, (b) 6 BV/h, (c) 9 BV/h.

Table 4. Parameters predicted from the Thomas and Yoon-Nelson models for L-trp adsorption

Flow rate (mL/min)	Thomas model			Yoon-Nelson model			R^2
	K_{Th} (mL g^{-1} min^{-1})	q_{the} (mg/g)	q_{exp} (mg/g)	K_{YN} (min^{-1})	τ_{the} (min)	τ_{exp} (min)	
0.962	1.31	703.2	705.8	0.013	384.3	380	0.918
1.182	1.48	697.5	672.7	0.015	310.2	310	0.900
1.348	4.87	449.0	405.8	0.049	175.1	172	0.966

study.

3. Column Desorption of L-trp by Eluant

After an eluant is chosen for desorption of L-trp, the concentration and flow rate of eluant are the important factors affecting the elution and recovery performance. After preliminary study (data not shown), aqueous ammonia was used as the eluant due to its validity and low cost. The L-trp concentration curves eluted by aqueous ammonia for HZ-001 are shown in Fig. 2. The feed concentrations of ammonia changed from 0.5 M to 2.0 M, and the flow rates were varied from 3 BV/h to 9 BV/h. The elution profiles showed that desorption of L-trp was dependent on the concentration of aqueous ammonia as well as the flow rate. The elution volumes exceeded 225 mL (15 BV) at aqueous ammonia concentration of 0.5 M, with the peak concentration of L-trp no more than 45.0 g/L. As the ammonia concentration increased, the elution volumes decreased markedly and the peak concentration rose due to the increasing desorption rate. Meanwhile, the peak shape was more symmetrical and spiculate at higher eluant concentration. However, a preliminary experiment indicated that a high concentration of ammonia would enhance the desorption rate of L-trp from column, resulting in column blockage. Meanwhile, the peak concentration and shape were highly dependent on the elution velocity. By comparison of the elution velocity in Fig. 2, L-trp was more concentrated (more spiculate in peak shape) at lower elution velocity for each concentration of ammonia, which was favorable for the successful separation of L-trp. Considering the peak shape and elution period, 2.0 M aqueous ammonia at the elution velocity of 6 BV/h was selected for this study.

The total amount of L-trp was obtained from integrating the effluent concentration with respect to time. The amount of L-trp released in the exit solution was in good agreement with that of L-trp adsorbed in the resin, which indicated that the elution by aqueous ammonia was complete.

4. Identification of the Reutilization of Column

To demonstrate the reusability of the HZ-001 resin, the adsorption-elution-regeneration cycle was performed. As shown in Fig. 3, after five cycles the bed capacity was about 95.5% of the initial value. This demonstrated that not only the adsorption capacity remained almost the same as the first operation, but also the elution and regeneration in each cycle were complete. Consequently, the stable column performance and effective operation procedure ensured its application in actual separation of L-trp from solution mixtures.

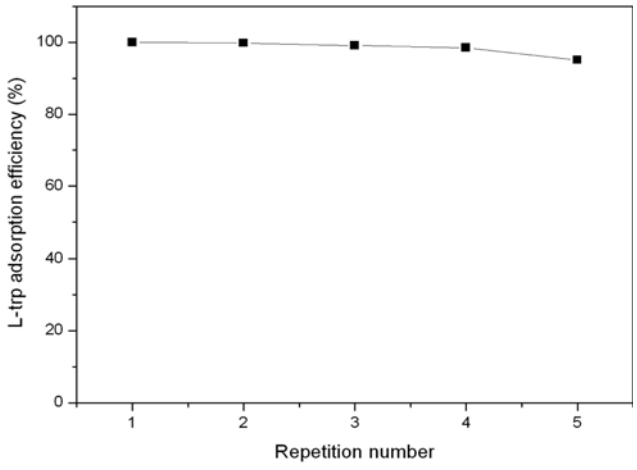

Fig. 3. Successive adsorbent reutilization of the HZ-001 packed column after continuous adsorption and elution steps.

CONCLUSIONS

The adsorption characteristics of L-trp in a fixed bed column filled with strong-acid cation resin HZ-001 were investigated. A number of theoretical models were adopted to describe the column performance. The theoretical models with the parameters properly identified were observed to predict reasonably well the experimental breakthrough curves. These models could significantly simplify the determination of column bed capacity and the breakthrough time of column adsorption process. Desorption of L-trp from column bed was optimized and the best elution profile was obtained with 2.0 M aqueous ammonia as eluant at 6 BV/h. The adsorption-elution-regeneration cycle was studied to determine the reutilization of the resin HZ-001. Results showed that the bed capacity was only reduced by 4.5% after 5 cycles, indicating that HZ-001 was an excellent adsorbent for L-trp recovery.

ACKNOWLEDGEMENTS

This work was financially supported by the National Natural Science Foundation of China (Grant No. 20736008), the Ministry of Science and Technology of China (National Basic Research Program of China, 2007CB707805) and the Natural Science Foundation of Zhejiang Province (Grant No. R4090041), the People's Republic of China.

REFERENCES

1. Z. N. Xu, Y. Chen, W. H. Shen and P. L. Cen, *Korean J. Chem. Eng.*, **23**, 108 (2006).
2. Y. Chen, H. B. Qu, Z. N. Xu and Y. Y. Cheng, *Korean J. Chem. Eng.*, **23**, 991 (2006).
3. D. Banerjee, M. A. Rao and S. K. Samanta, *Solvent. Extr. Ion. Exc.*, **26**, 687 (2008).
4. S. Melis, J. Markos, G. Cao and M. Morbidelli, *Ind. Eng. Chem. Res.*, **35**, 1912 (1996).
5. H. Nagai and G. Carta, *Sep. Sci. Technol.*, **39**, 3691 (2004).
6. S. Rengaraj, J.-W. Yeon, Y. Kim, Y. Jung, Y.-K. Ha and W.-H. Kim, *J. Hazard. Mater.*, **143**, 469 (2007).
7. M. H. L. Ribeiro, D. M. F. Prazeres, J. M. S. Cabral and M. M. R. d. F., *Bioprocess Eng.*, **12**, 95 (1995).
8. T. E. Köse and N. Öztürk, *J. Hazard. Mater.*, **152**, 744 (2008).
9. F. Alguacil, M. Alonso and L. Lozano, *Chemosphere*, **57**, 789 (2004).
10. M. J. Ahmed, A. H. A. K. Mohammed and A. A. H. Kadhum, *Korean J. Chem. Eng.*, **27**, 752 (2010).
11. V. C. Srivastava, B. Prasad, I. M. Mishra, I. D. Mall and M. M. Swamy, *Ind. Eng. Chem. Res.*, **47**, 1603 (2008).
12. R. Han, D. Ding, Y. Xu, W. Zou, Y. Wang, Y. Li and L. Zou, *Bioresour. Technol.*, **99**, 2938 (2008).
13. W. Luo, H. Chen, L. Fan, J. Huang, L. Huang, Z. Xu and P. Cen, *Korean J. Chem. Eng.*, DOI:10.2478/s11814-010-0490-2.
14. J. R. Rao and T. Viraraghavan, *Bioresour. Technol.*, **85**, 165 (2002).

15. Z. Aksu, F. Gönen and Z. Demircan, *Process. Biochem.*, **38**, 175 (2002).
16. A. C. Texier, Y. Andres, C. Faur-Brasquet and P. LeCloirec, *Chemosphere*, **47**, 333 (2002).
17. Z. Aksu and F. Gönen, *Process. Biochem.*, **39**, 599 (2004).
18. D. O. Cooney, *Chem. Eng. Commun.*, **110**, 217 (1991).
19. P. Malakul, D. Srinivasan and H. Y. Wang, *Ind. Eng. Chem. Res.*, **37**, 4296 (1998).
20. S. Lin, *Chem. Eng. J.*, **92**, 193 (2003).
21. S. H. Lin and C. S. Wang, *J. Hazard. Mater.*, **B90**, 205 (2002).
22. V. Sarin, T. Singh and K. Pant, *Bioresour. Technol.*, **97**, 1986 (2006).
23. X. Liao, M. Zhang and B. Shi, *Ind. Eng. Chem. Res.*, **43**, 2222 (2004).
24. Y. H. Yoon and J. H. Nelson, *Am. Ind. Hyg. Assoc. J.*, **45**, 509 (1984).
25. W. T. Tsai, C. Y. Chang, C. Y. Ho and L. Y. Chen, *J. Hazard. Mater.*, **69**, 53 (1999).
26. P. Ye, Z. Luan, K. Li, L. Yu and J. Zhang, *Carbon*, **47**, 1799 (2009).